PAPER

Check for updates

A novel poly(acrylonitrile)/poly(ethylene glycol)-based polymer gel electrolyte for high efficiency dye sensitized solar cells†

Madhu Mohan Varishetty, [ID] *[ab] Murakami Kenji,[c] Nazia Tarannum, [ID] [d]
Srinivasa Rao Damaraju[e] and Madhavi Jonnalagadda[f]

This research article reports on a systematic approach to the development of polymer gel electrolytes (PGEs) for the applications of dye-sensitized solar cells (DSSCs). The authors prepared PGE blend using poly(acrylonitrile) (PAN) and poly(ethylene glycol) (PEG) polymers along with three different ionic salts. They demonstrated a good ionic conductivity of 1.52×10^{-2} S cm^{-1}, which improved PV performance. The conduction mechanism of the (PAN/PEG) PGE is based on the interaction of three cations of distinct sizes, Hex_4N^+, K^+, and Li^+ ions, with the polymer host. The rapid diffusion of I^-/I_3^- iodide ions through the pores formed by PEG in the PGE is the primary cause of improved ionic conductivity. Various compositions of (PAN/PEG) have been optimized to obtain a sufficient porous structure and improved photon conversion efficiency (PCE) of the cell, achieving 8.6% in this research. X-ray diffraction (XRD), field emission scanning electron microscopy (FE-SEM), impedance spectroscopy, incident photon conversion efficiency (IPCE) and finally current density voltage ($J–V$) characterization techniques are used to analyze and compare the results with those of liquid electrolyte-based cells.

1. Introduction

It is widely appreciated that dye-sensitized solar cells are among a wide variety of photovoltaic devices, such as thin-film solar cells, hetero-junction solar cells and dye-sensitized solar cells (DSSCs). DSSCs are most suitable due to their scalability, low-cost fabrication and satisfactory efficiency. Hence, these have been rapidly developed to meet the demands of the next generation of sustainable energy sources of future photovoltaics.[1–3] Among all types of DSSCs, such as solid, liquid and gel electrolyte, we are primarily interested in gel DSSCs due to their inadequately addressed drawbacks.

DSSCs based on liquid electrolytes showed a photoelectric conversion efficiency of up to 11% with the presence of triiodide/iodide (I_3^-/I^-) as a redox couple.[4] DSSCs made using liquid electrolytes raise various practical problems such as

solvent evaporation (typically prepared by using volatile organic solvents), flammability, leakage due to long-term operation, desorption of weakly adsorbed dyes and corrosion of electrodes.[5,6]

Solid polymer electrolytes showed better stability without leakage of electrolyte solution in the devices. However, they exhibited low ionic transport and weak interfacial contact between the electrolyte and the mesoporous TiO_2 photoelectrode. Therefore, the DSSCs made with solid polymer electrolytes showed lower fill factor and short-circuit current values. Hence, the solid-state DSSCs show a decrease in energy conversion efficiency compared to the liquid electrolyte-based devices.[7,8]

To address these drawbacks, organic hole-conducting transport materials, an *in situ* photopolymerization method[9] and p-type semiconductors were introduced to overcome the critical sealing procedures in the fabrication of DSSCs. These materials exhibit more stability in DSSCs. However, the poor wettability of TiO_2-coated electrodes caused by these electrolytes results in poor conductivity, thereby decreasing the efficiency of the cells.[10]

PGEs partially have the properties of both liquid and solid electrolytes and offer improved long-term stability over DSSCs. PGEs show better mechanical properties, minimized electrolyte evaporation, low production cost, easy synthesis, excellent ionic conductivity and more efficient trapping of the liquid

[a] *Research institute of Electronics, Shizuoka University, Hamamatsu, Japan.*
  E-mail: madhuvm123@yahoo.com
[b] *Mohan Babu University, Tirupathi, Andrapradesh, India*
[c] *Graduate School of Engineering, Shizuoka University, Hamamatsu, Japan*
[d] *Department of Chemistry, Chaudhary Charan Singh University, Meerut, Uttar Pradesh, India*
[e] *IIIT-AP Ongole campus, Rajiv Gandhi University of Knowledge Technologies, India*
[f] *Indian Institute of Science, Banglore, India*
† Electronic supplementary information (ESI) available. See DOI: https://doi.org/10.1039/d3ya00079f

electrolyte.[11] PGEs are more suitable due to their higher thermal stability, low vapour pressure and filling ability between the electrodes in DSSCs.[12–14]

PGEs are prepared by using a polymer host that comprises ionic liquids in its cages and forms a network like a three-dimensional structure. In these liquid phases of the polymer network, ions can move freely, which provides a major contribution to the ion conductivity of a PGE. Several polymers were used for the fabrication of dye sensitized solar cells, *viz.*, poly(ethylene glycol) gel polymer electrolytes with heteroleptic cobalt redox shuttle and pyridine,[15] PEG-functionalized ABA triblock copolymers,[16] PEG and PVA polymers for gel electrolytes,[17] poly(ethylene glycol) and polyvinylidene fluoride,[18] poly(ethylene glycol),[19] polyethylene glycol/4,4′-diphenylmethane diisocyanate copolymers,[20] PEG-based ABA triblock copolymers,[21] polyethylene glycol based quasi-solid state electrolytes,[22] ionic liquid integrated polyethylene glycol (PEG)-based quasi-electrolytes,[23] polyaniline integrated poly(hexamethylene diisocyanate tripolymer/polyethylene glycol) gel electrolytes,[24] PAN-based triblock copolymers,[25] poly(acrylonitrile) gel polymer electrolytes for prototype solar panels[26] and poly(acrylonitrile-*co*-vinyl acetate)[27] PGEs for DSSC applications.

S. Balamurugan[15] and R. S. Seni[17] *et al.* demonstrated PEG polymer hosts, which lead to improved conductivity and efficiencies of the DSSCs due to its higher rate of polarization, greater chemical stability, and it has the ability to easily dissolve redox couples. Therefore, poly(ethylene glycol) (PEG) has a lot of potential for application in the preparation of PGEs. However, pure PEG polymer electrolytes have limited ionic conductivity compared to PEG/1-N-BHII polymer electrolytes due to low charge transportation and a lower diffusion coefficient.[17,28] Therefore, additional treatment/modification is necessary to improve their properties. In order to reduce the sublimation of iodine, heteroatoms with lone pair electrons such as nitrogen, oxygen, and sulphur atoms are utilized for the formation of a charge transfer complex with iodine.[5] The addition of 4-tetra-butyl pyridine (TBP) and guanidinium thiocyanate (GuSCN) to the polymer host maintains TiO$_2$'s downward displacement and negative potential shift.[21] In order to improve cell efficiency, Pugliese *et al.*[29] demonstrated flexible back-illuminated DSSCs with TiO$_2$ nanotube photoanodes. Bist *et al.*[30] and Ahmad *et al.*[31] utilized natural extract-mediated and natural food dyes for DSSCs.

PAN gel electrolytes showed low ionic conductivity due to their strong dipole–dipole interactions. The high-dielectric constant materials such as ethylene carbonate (EC) and propylene carbonate (PC) were added to PAN, to improve the GPE properties as reported in the literature.[32–35] Because of its high electrochemical stability, insect resistance, easily solvable cations, and high abrasion resistance, poly(acrylonitrile) (PAN) is used in our current work. Hence, it has been extensively utilized as a polymer host to prepare PGEs for DSSCs.[7,19,32–36] In order to avoid the individual drawbacks of PEG or any other single polymer, blending systems have been developed like the PEG-PAA hybrids[37] and PEG/PMMA blends[38,39] for DSSCs.

The effect of binary salts on conductivity and solar cell efficiencies has been discussed as follows. The small size iodide salt can adsorb on the surface of TiO$_2$ easily; due to its smaller ionic radius, the conduction band edge is shifted, and therefore open circuit voltage decreases.[40] The distance between the LUMO level and the conduction band decreases, leading to an increase in electron generation from the dye to TiO$_2$. Hence short circuit current density increases (J_{sc}). In the case of a bulky iodide salt, it dissociates easily into free ions due to its lower lattice energy than smaller cations. Hence bulky cation iodide salts exhibit high ionic conductivity and also help in retarding the backward electron transfer from TiO$_2$ to I$_3^-$.[41] Therefore binary salts exhibited better DSSC performance than single iodide salts. In addition to this, a combination of three iodide systems of lithium iodide (LiI), 1-butyl-3-methylimidazolium iodide (BMII), and tetrapropylammonium iodide (Pr4NI) has been investigated for polymer gel electrolytes in DSSCs.[42] The authors suggested that various individual ions played different roles in improveing solar cell efficiency. Pr4NI increased J_{sc} by increasing the ion transport number. An imidazolium ionic liquid contributed to the enhancement of V_{oc} due to its plasticizing effect. Therefore authors suggested that ternary iodides employing quasi-solid-state DSSCs exhibited improved efficiency (η) by 30% and current density (J_{sc}) by 62%.

To continue these efforts, we have prepared a PAN/PEG polymer blend gel electrolyte for the improvement of conductivity by creating a porous gel electrolyte along with the synergetic effect of a triple mixture of LiI, KI, and 1-*n*-butyl-3-hexyl imidazolium iodide exhibiting three different cation sizes (Hex4N$^+$, K$^+$, and Li$^+$) for the enhancement of the efficiency of DSSCs. We have explained clearly the working mechanism of the prepared gel in the DSSCs.

2. Experimental section

(a) Preparation of the dye-sensitized nanoporous TiO$_2$ photoelectrode bottom layer

Initially, fluorine doped tin oxide (FTO) transparent conductive glass (FTO 10–15/Asahi Glass, Japan) was extensively cleaned using acetone, followed by ethanol. The spray pyrolysis experimental technique was introduced to prepare TiO$_2$ working photoelectrodes using a colloidal solution consisting of smaller size particles (3–5 nm) in a 2.2% suspension, supporting previous literature.[43–46] Later, 0.3 g of P-25 TiO$_2$ powder was taken into a ceramic mortar and mixed with 5.5 mL of acetic acid, followed by grinding without any agglomeration of particles. Then, these solutions were mixed with a colloidal TiO$_2$ solution (20 mL) and allowed to ultrasonically vibrate for about 30 min after adding 5 drops of Triton X-100. This solution was sprayed onto FTO glass plates with an active area of 0.25 cm^2 and kept at a constant temperature of 150 °C for 30 min before being sintered in a hot air oven at 500 °C for 30 minutes. Then, the samples were slowly cooled down to room temperature. TiO$_2$ spray-coated plates were immersed in N-719 dye for

adsorption. Similarly, we prepared another photoelectrode by using the synthesised 450 nm-sized TiO_2 nanospheres, which were coated as a scattering layer along with the colloidal solution to obtain a bilayer configuration that exhibited good efficiency in solar cells. We made all of the photoelectrodes of the same thickness of 23 μm.

(b) Synthesis of TiO_2 spheres used as a top scattering layer

Initially, titanium tetrasopropoxide (TTIP) (6.0 mmol, Wako) was drop-wise stabilised in ethanol (10 mL, Aldrich). Second, another solution was prepared separately by mixing ethanol (50 mL), acetonitrile (40 mL, Aldrich), methylamine (1.0 mmol) and water (24 mmol). When both solutions were mixed, they turned milky within a few seconds. The resulting suspension was stirred for about 1 h to get TiO_2 microspheres. The amorphous TiO_2 spheres were collected using a centrifuge, washed with ethanol, then transferred to an autoclave. The autoclave was filled with 30 mL of ethanol/water (1:1) along with spheres and kept in an hot oven at 240 °C for 6 h. The product was washed several times using ethanol and dried. By maintaining methylamine (CH_3NH_2) as a constant and changing the TTIP/water molar ratios spheres with varying diameters can be produced. Spheres of various diameters, which are fine nanoparticles, were synthesized.[47]

(c) Preparation of PGE

The components of quasi-PGE are PC (0.750 g), EC (0.525 g), 1-n-butyl-3-hexyl imidazolium iodide ($Hex4N^+I$) (0.249 g), PAN (0.225 g), I (0.008 g), LiI (0.0325 g), poly(ethylene glycol) (PEG 20,000) and KI (0.0150 g). The redox species composition was also optimized in the electrolyte medium. The addition of each component to the polymer was accompanied by ultrasonic vibration to get an appropriate PGE. The resulting mixture was heated to around 120 °C and stirred until it formed a viscous gel. The prepared viscous gel was placed between two glass plates and a film thickness of about 50 μm was obtained. In order to prevent moisture absorption, films were stored in desiccators. Fig. 1(a) and (b) show the schematic representation of the prepared PGE and the distribution of various ions in the film, respectively.

(d) Solar cell fabrication

Polymer gel electrolyte was cut as required to cover the TiO_2 photoanode area of 0.25 cm^2. It was placed on top of the TiO_2 photoanode area by positioning the polymer gel electrolyte on the counter electrode platinum side and aligning them together on the photoanode TiO_2 surface. In other words, the gel electrolyte film was arranged as an intermediate layer between the photoanode and counter electrodes. The as prepared DSSCs based on PAN/PEG polymer blend gel electrolytes were sealed and used for various characterization studies, such as impedance and JV measurements.

(e) Characterization techniques

The Rigaku RINT Ultima-III X-ray diffractometer was used for the XRD measurement with an angle of 2θ over the range of
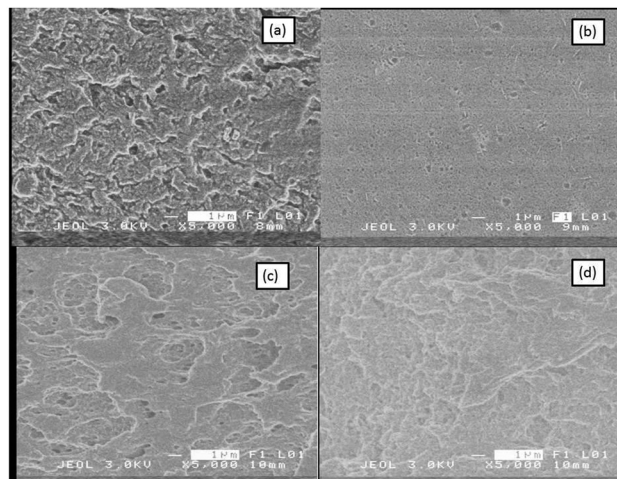

Fig. 1 (a) and (c) FE-SEM pictures of the surface and cross-sectional view of the PAN/PEG/LiI/KI blend. (b) and (d) Images related to dried PAN/LiI/KI PGEs films.

10 to 70 degrees. A field emission scanning electron microscope (FE-SEM), JEOL JSM-7001F, was used to measure the surface morphology of the PGE films and prepared spheres. The ionic conductivities of PGEs were measured through complex impedance measurements. FRA 5022 and HZ-5000 automated polarization systems (Hokuto Denko, Japan) were utilized to perform impedance measurements through a frequency response analyzer. A calibrated JASCO CEP- 25 BX solar cell system was used to obtain measurements of current density $vs.$ voltage (J–V) and incident photon to current conversion efficiency (IPCE). All measurements were taken at room temperature in the Shizuoka University RIE laboratory.

3. Results and discussion

3.1. X-Ray diffraction

The X-ray diffraction patterns of the as prepared samples of PGEs were measured using (a) PAN/LiI/KI and (b) PAN/PEG/LiI/KI, as shown in the ESI,† Fig. S1. Fig. S1 (ESI†) shows an increase in the degree of amorphocity at a specified concentration (0.0150 g) of KI when added to PAN/PEG/LiI as compared to the non-blended PAN/LiI polymer sample. A widened peak has appeared in all the samples, indicating that the peak belongs to the polymer host in the range of 20°–30°.[7,44] The entire XRD pattern shows a mostly amorphous nature, indicating the appropriate mixing of the ingredients to form a gel electrolyte. Yang $et\ al.$[48] reported that the decrease in the degree of crystallinity is due to the miscibility of all the components, producing a homogenous phase in the blended PGEs, supporting our data. It is well known that the dominant presence of amorphous nature is due to the increased polymer chain flexibility, which enhances electrical conductivity.

3.2. Morphological analysis

Fig. 1(a) and (c) show field emission scanning electron micrographs of PAN/PEG/LiI/KiI blend PGE dried films, illustrating

the surface and cross-section, respectively. The surface and the cross-section of the film have numerous random pores, which could be created by PEG-rich domains throughout the film. PEG-rich domains are created at higher concentrations of the solvent; therefore, inside the polymer films, coalescence does not occur. The coalescence of the separated PEG-rich domains in the phase was very active at low solvent concentrations, possibly due to the high viscosity of the polymer matrix during the phase separation process. Because of the low viscosity of the polymer matrix, the rich PEG droplets balanced the surface tension[49] by floating on the air–solution interface and then precipitated, descending in the vessel due to their high density. Some of the precipitated droplets descended and created pores inside the polymer during the drying process. In our previous report,[50] we optimized all solvent conditions along with PAN/PEG ratios to achieve the best efficiency of the DSSC. Fig. 1(b) and (d) show relatively less porosity on the surface and in the cross-section, respectively, as a characteristic feature of single polymers PAN/LiI/KiI.

Fig. 2(a) shows the prepared 450 nm diameter spheres of TiO$_2$, while Fig. 2(c) shows the top view of the photoelectrode with spray-coated spheres as the top layer. Fig. 2(b) shows the cross-section of the photo-electrode, where the first layer about 15 μm as indicated as X in Fig. 2(b) is sprayed on the FTO surface with P25/colloidal solution, followed by the second layer Y of about 8 μm thickness deposited using 450 nm spheres/colloidal solution. The magnified image in Fig. 2(d) indicates good contact between the spheres as a result of mixing of Tyco colloidal solution during the spray pyrolysis method. These connections formed by the colloidal solution particles in between the spheres enhance the electrical conductivity by increasing the charge transfer rate of the photoelectrode[47] and offer excellent light harvesting efficiency as the microspheres act as a good scattering layer.[51]
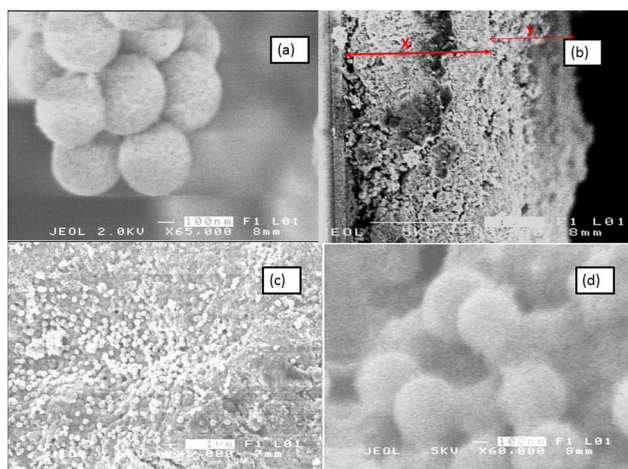

Fig. 2 (a) Synthesized spheres of about 450 nm diameter. (b) Bilayer photo-electrode composed of P25 and colloidal solution mixture first layer/spheres and colloidal solution second layer (c) Top view of the sphere-coated photoelectrode. (d) Clear view of sprayed colloidal particle attached to the spheres.

3.3. Electrical conductivity

Complex impedance measurements were used to find the electrical conductivity of the (PAN/PEG) polymer blend gel electrolyte at ambient temperature. The ionic conductivities of polymers were evaluated using the relation

$$\sigma = l/R_b \cdot A \qquad (1)$$

where R_b is the bulk resistance, l is the thickness and A is the contact area of the electrode with the electrolyte film during the experimentation. The bulk resistance (R_b) is calculated from the intercept made by the impedance plot with the real axis. The increase in conductivity caused by blending of the polymer is beneficial for the enhancement of photon energy conversion into electrical power efficiency.[52,53] The important ionic conductivities of PAN/LiI, PAN/PEG/LiI and PAN/LiI/KI PGEs are found to be 1.16×10^{-3} S cm^{-1}, 5.06×10^{-3} S cm^{-1} and 6.93×10^{-3} S cm^{-1}, respectively, while ionic conductivity of PAN/PEG/LiI/KI PGE was obtained as 1.57×10^{-2} S cm^{-1}. This reveals that blending of the polymer with optimized inorganic two salts yields higher electrical conductivity.

3.4. Conduction mechanism in the as-prepared (PAN/PEG) polymer blend gel electrolyte

In the first step, the blend matrix shows a porous structure, which helps in easy ionic movement. However, the coalescence of PEG domains is the dominant factor in the creation of the final porous morphology. The liquid–liquid phase separation occurs early on and the solvent may crystallize. As a result, when droplets form, PEG precipitates easily and aggregates until the solvent crystallizes completely. Therefore, the coalescence of PEG domains in the polymer solution was controlled by its viscosity. The concentration of the solvent is reduced due to its crystallization. Hence, the surface and cross-section of the film have numerous random pores apparent in the microstructure due to the evaporation of the solvent. Na *et al.* reported a similar porous electrolyte for super-capacitors.[54] The large amount of liquid electrolyte present in the pores or cages of the gel favorably allowed easy transport of ions due to its lower viscosity compared to solids, thereby increasing the ionic conductivity. Fig. 3(a) and (b) show a systematic presentation of the conduction mechanisms of PAN/KI/LiI and PAN/PEG/KI/LI polymer gel electrolytes. The blending of PEG and PAN can result in the formation of pores containing solvents that are favorable for ion (I$^-$ and I$_3^-$ ions) transportation due to a shorter diffusion distance compared to PAN/LiI/KI polymer gel electrolytes.

In the second step, the addition of 1-*n*-butyl-3-hexyl imidazolium iodide (Hex$_4$N$^+$I$^-$) increases the polymer conductivity, indicating that the number of ion mobile charge carriers increases. This is due to the high rate of salt dissociation and the lower lattice energy of Hex$_4$N$^+$I$^-$ compared to KI and LiI. In other words, the presence of bulky cations in Hex$_4$N$^+$I$^-$ increases the lattice energy by decreasing the salt dissociation rate. Similarly, KI salt also decreased the flexibility of the polymer and decreased the mobility of ions due to its strong
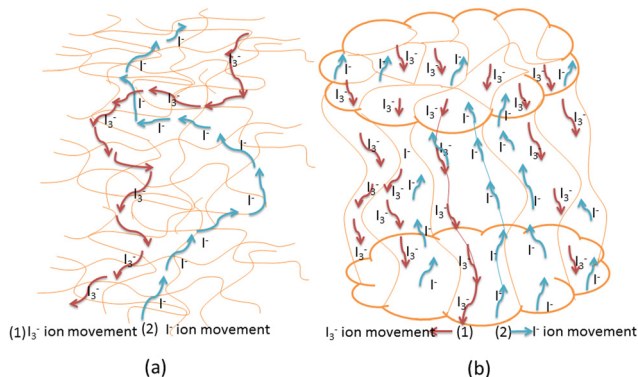
Fig. 3 Conduction mechanism of (a) PAN/LiI/KI and (b) PAN–PEG/LiI/KI blend PGEs.

cross-linking effect on the long chain.[55] The higher charge density of the K^+ cation promotes cross-linking between the CN groups of PAN chains in the polymer. This improves the ionic conduction of the mixture of these components comprising gel electrolyte by increasing iodine ion diffusion and thus enhances the performance of the DSSCs.[56] When the bigger ions ($Hex_4N^+I^-$) enter between polymer chains, they cause expansion at some other places, while smaller Li^+ and K^+ ions are randomly present at various positions, creating more disorder in the electrolyte. Hence, long polymer chains are separated appreciably by enhancing the flexibility of the polymer as compared to LiI and KI salts. Li^+ ions of smaller size (0.76) can easily move through the wider space created by larger ions of $Hex_4N^+I^-$ and K^+. Hence, GPEs exhibited higher conductivity. The distribution of ions in the (PAN/PEG) polymer blend host and the as-prepared polymer gel electrolyte films is shown in Fig. 4a and b, respectively.

3.5. IPCE measurements

Fig. 5 reveals the comparison of the incident photon conversion efficiency (IPCE) measurements of the DSSCs of liquid, PAN and PAN/PEG polymer gel electrolytes. IPCE is stated as the ratio of the generated electrons across the external circuit
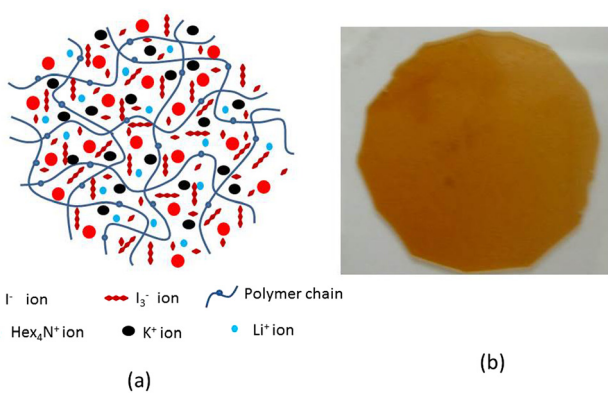

Fig. 4 (a) Schematic representation of the distribution of doping ions in the PAN/PEG blended PGE. (b) Physical appearance of the as prepared PGE using the hot pressing method.
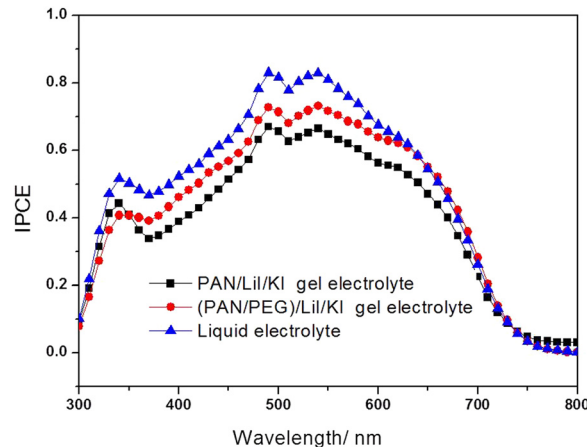

Fig. 5 The IPCE curves for DSSCs based on liquid electrolyte, PAN/LiI/KI and PAN/PEG/LiI/KI blend PGEs.

($n_{electrons}$) to the injected photons ($n_{photons}$) using the relation

$$\text{IPCE}(\lambda) = \frac{n_{\text{electrons}(\lambda)}}{n_{\text{photons}(\lambda)}} = \frac{1240 I(\lambda)}{\lambda \phi(\lambda)}$$

where $\phi(\lambda)$ indicates the incoming power at a wavelength and $I(\lambda)$ represents the cell current at that wavelength. Fig. 5 reveals that the PAN/PEG/Li/KI gel polymer electrolytes based on DSSCs showed higher quantum efficiency as compared to the PAN/Li/KI gel polymer electrolyte. However, due to the lack of interfacial contact, the efficiency is lower than that of a liquid electrolyte.[57] The PAN/PEG/Li/KI gel electrolyte has higher ion conduction and lower viscosity compared to the PAN/Li/KI polymer gel electrolyte, which enhances the quantum efficiency to about 18.2% at 400 nm and to 21.6% at around 650 nm wavelengths. The IPCE measurement was carried out with the same system used for J–V characteristics, but the data were obtained under monochromatic light by using a xenon-lamp (model PS-X500). The enhancement of interfacial contact between the photoelectrode and the electrolyte layer is due to electrolyte penetration into the photoelectrode of the DSSCs. The increasing ionic conductivity[16,58,59] of the polymer gel as revealed by impedance measurements resulted in a higher IPCE of DSSCs.

3.6. Analysis of electrochemical impedance spectroscopy (EIS)

EIS was used to determine the interfacial properties of the components, charge transport and kinetic recombination in DSSCs.[60,61] The EIS plot of DSSCs prepared using a sprayed TiO_2 photoelectrode, PAN, PAN/PEG blend PGEs or liquid electrolyte, and a Pt counter electrode is shown in Fig. 6. The presence of FTO resistance in DSSCs may have caused the observation of series resistance (R_2 = 14.77) in the high-frequency range. Each plot comprises three semicircles in different frequency ranges. The resistance R_{ct1} indicates the charge transfer resistances present at the interface between the gel electrolyte/liquid electrolyte and the counter electrode. R_{ct2} represents the resistance at the interface present between the gel electrolyte/liquid electrolyte and the photoelectrode. Z_w
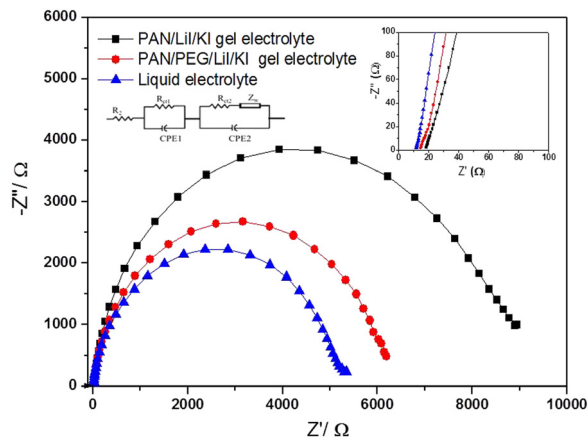
Fig. 6 The impedance spectra of the DSSC based on liquid electrolyte, PAN/LiI/KI and PAN/PEG/LiI/KI blend PGEs. The inset plot shows the contact resistance between the electrolyte and the Pt electrode interface.

Fig. 7 Schematic representation of the deigned DSSC model with various components.

denotes the Warburg impedance caused by I^-/I_3^- redox couple diffusion in the polymer electrolyte.[5,61] This Warburg impedance may be lower for PAN/PEG/LiI/KI gel electrolytes than for PAN/LiI/KI PGEs and also low for liquid electrolytes. Nyquist plots comprise a semicircle, which reveals series resistance values (R_2) and various impedance parameters, as indicated in Table 1. The charge transfer resistance in the second semicircle decreases from 8.89 kΩ to 6.24 kΩ due to the blending of PEG with PAN as a polymer host, which enhances the charge transport from the counter electrode to the TiO2 electrode. The Warburg impedance (Z_w) of PAN/PEG blend gel electrolyte-based DSSCs showed a lower value of 3.257 kΩ compared to the PAN single PGE, resulting in a higher efficiency of 8.62%.

3.7. J–V characteristics

The schematic representation of our fabricated DSSC based on PAN/PEG blend GPE is shown in Fig. 7. The photovoltage produced by a DSSC is primarily determined by the electron transfer process of the redox couple (I^-/I_3^-). The development of open-circuit voltage in DSSC devices mainly depends on the potential difference between the Fermi level electrons in the TiO2 photoelectrode and the redox potential of the electrolyte.[62,63] The chemical reaction of the I^-/I_3^- redox couple is represented in eqn (2)–(4). In the case of the counter electrode, the triiodide ions accept electrons on the electrolyte/FTO glass surface and are oxidized into iodide ions, represented in (eqn (2)). These iodide ions participate in the regeneration of ground-state dyes by providing electrons to the positively charged dye, as indicated in eqn (3):

$$I_3^- + 2e \rightarrow 3I^- \quad (2)$$

$$3I^- + 2dye^+ \rightarrow I_3^- + 2dye \quad (3)$$
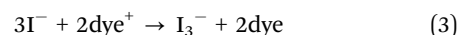
$$V_{oc} = \frac{kT}{q} \ln\left(\frac{\eta \Phi_0}{n_0 k_{et}[I_3^-]}\right) \quad (4)$$

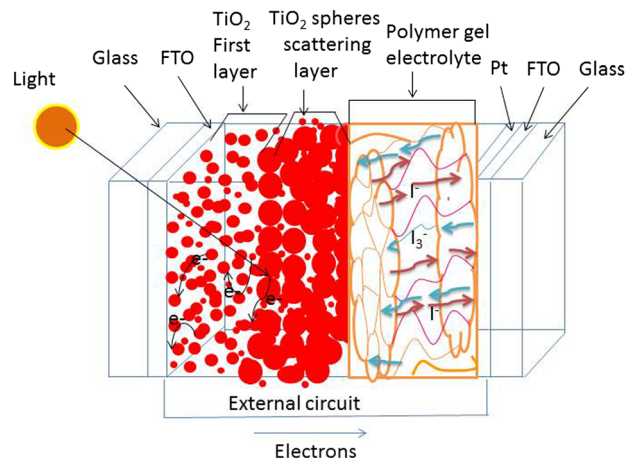In eqn (4), η indicates the quantum efficiency of the photo-generated electrons due to the incident photon flux of (Φ_0). The
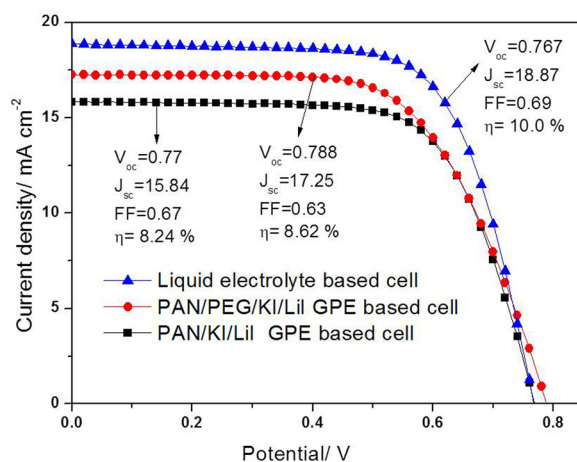

Fig. 8 Photo-current density–voltage characteristics (J–V) of DSSCs based on liquid electrolyte, PAN/LiI/KI and PAN-PEG/LiI/KI blended PGEs using an illuminated light intensity of 100 mW cm⁻².

Table 1 The fitted impedance parameters for the liquid electrolyte, PAN/PEG/LiI/KI and PAN/LiI/KI GPEs based DSSCs

No.	Electrolyte	R_s (Ω)	R_{ct1} (Ω)	R_{ct2} (kΩ)	Z_w (kΩ)
1	Liquid electrolyte	11.73	23.52	5.201	1.025
2	PAN/PEG/LiI/KI GPE	14.77	35.37	6.244	3.257
3	PAN/LiI/KI GPE	18.49	39.61	8.897	5.986

Table 2 Photo current density–voltage characteristics of liquid electrolyte, PAN/PEG/KI/LiI and PAN/LiI/KI based DSSCs under 100 mW cm⁻² illumination

Name of the sample	V_{oc} (V)	J_{SC} (mA cm⁻²)	FF	Efficiency (%)
Liquid electrolyte	0.754	18.31	0.66	9.11
PAN/PEG/LiI/KI polymer gel electrolyte	0.772	16.83	0.62	8.15
PAN/LiI/KI polymer gel electrolyte	0.764	15.62	0.63	7.56

Table 3 Comparison of current GPE with various GPEs already reported

S. no.	Polymer gel electrolyte	Conductivity (S cm^{-1})	Efficiency (%)	Ref.
1	PAN-EC-PC-KI-TPAI-I$_2$	3.28×10^{-3} (25 °C)	4.93	35
2	PAN-EC-PC-TPAI-KI-I$_2$	2.8×10^{-3} (27 °C)	5.36	69
3	PAN-EC-PC-TPAI-MgI$_2$-I$_2$	1.08×10^{-3} (27 °C)	5.18	70
4	PAN-EC-PC-LiI-THAI-I$_2$	2.75×10^{-3} (27 °C)	4.2	71
5	PAN-gBL-LiI-NMBI-GuSCN-DMPII-I$_2$	2.41×10^{-3} (27 °C)	7.68	72
6	PAN-EC-PC-NaI-HMII-I$_2$	6.72×10^{-3} (25 °C)	5.75	73
7	PAN/PEG-EC-PC-Hex4N + I-KI-LII	1.52×10^{-2} (27 °C)	8.6	Current

electron concentration was represented by n_0 under a dark condition, while k_{et} indicated the rate of recombination for a given triiodide concentration [I$_3^-$].

In contrast, with the increasing PEG content in PAN/PEG, the open circuit voltage (V_{oc}) of the DSSCs increases rapidly, as mentioned in the previous report.[47] The formation of the cross-linked polymer on the TiO$_2$ photoelectrode surface reduces the back-transfer of electrons from the conduction band of TiO$_2$ to the I$_3^-$ ion in the electrolyte. Hence, the V_{oc} of the cell improved.[64]

The J–V curves of the DSSCs consist of double-layered and mono-layered TiO$_2$ photo-anode assemblies based on PAN, PAN/PEG, PGEs, and liquid electrolytes, as shown in Fig. 8. The cell parameters of DSSCs fabricated using a TiO$_2$ photo-anode with different gel and liquid electrolytes are shown in Table 2. While blending the higher concentrations of PEG, a higher cross-linking effect between PEG, PAN, Hex$_4$N$^+$, K$^+$ and Li$^+$ ions arises, which lowers the ionic conductivity and thereby leads to poor conversion efficiency. Therefore, blending of PEG at an optimal concentration is required for good conversion efficiency.

Ahn et al.[65] performed electrophoresis measurements and reported that the dye-adsorbed TiO$_2$ film cannot adsorb bulky cations such as Bu$_4$N$^+$ and Hex$_4$N$^+$. Novelli et al.[66] revealed that the adsorption of cations on the surface of TiO$_2$ can reduce the electron injection rate, thereby decreasing the quantum efficiencies of the DSSCs. The acceptor states in TiO$_2$ would shift due to the adsorption of surface cations. The cation behaviour was described by the electrostatics at the interface between the semiconductor and electrolyte. The efficient interfacial charge injection is attributed to the presence of more positive electrochemical potentials.[67]

We determined the concentration of Hex$_4$N$^+$, K$^+$ and Li$^+$ ions in our electrolyte system, and observed their effect on the variation of J_{SC}, V_{oc} and efficiency of the solar cells. In addition, the smaller lithium ions enter easily into the TiO$_2$ surface or lattice, thereby changing the concentration of electrons in the TiO$_2$ crystal. The photocurrent and voltage of the DSSCs change as the lithium ion concentration in the electrolyte system increases with an increase in LiI salt. However, the quasi-solid-state DSSC performance increased by increasing its iodide ion conductivity.[68] In our PAN/PEG/LiI/KI gel electrolyte system, numerous random pores offer a fast iodide diffusion rate, which enhances electrical conduction. The comparison of the current electrolyte with reported data is given in Table 3. The presence of three different kinds of cations Hex$_4$N$^+$, K$^+$ and Li$^+$

in the electrolyte system can affect the performance of DSSCs. The ionic conductivity increases with increasing of cation size while decreasing cation size decreases the electron injection as well as charge separation in the photo-electrode. Therefore, our results reveal that the GPE containing three mixed cations with different sizes (Hex$_4$N$^+$, K$^+$, and Li$^+$) shows excellent solar cell performance and better conductivity compared to a single or double cation system.

4. Conclusions

Dye-sensitized solar cells were fabricated with PGEs and a triple iodide system (Hex$_4$N$^+$, K$^+$, and Li$^+$) and their performance was evaluated. The PAN/PEG ratio and the concentration of triiodides have been optimized for achieving the best efficiency of solar cells. The blending of PEG with PAN as a polymer host played a vital role in decreasing the charge transfer resistance from 8.89 kΩ to 6.24 kΩ as indicated by the impedance studies. The high ionic conductivity in the gel state is attributed to the accumulation of a large amount of liquid electrolytes into the numerous random pores of PAN/PEG. A comparison between the parameters of the as-prepared DSSCs and those using liquid electrolytes was carried out. This electrolyte system showed a better electrical conductivity of 1.52×10^{-2} S cm^{-1} with an efficiency of about 8.62% which is best among those of polymer gel electrolyte systems.

Conflicts of interest

The authors declare that they have no known competing financial interests or personal relationships that could have appeared to influence the work reported in this paper.

Acknowledgements

References

1 H. Jiang, Y. Ren, W. Zhang, Y. Wu, E. C. Socie, B. I. Carlsen, J.-E. Moser, H. Tian, S. M. Zakeeruddin, W.-H. Zhu and M. Grätzel, Phenanthrene-fused-quinoxaline as a key

building block for highly efficient and stable sensitizers in copper-electrolyte-based dye-sensitized solar cells, *Angew. Chem., Int. Ed.*, 2020, **59**, 9324–9329, DOI: **10.1002/anie.202000892**.

2 Q. Huaulmé, V. M. Mwalukuku, D. Joly, J. Liotier, Y. Kervella, P. Maldivi, S. Narbey, F. Oswald, A. J. Riquelme, J. A. Anta and R. Demadrille, Photochromic dye-sensitized solar cells with light-driven adjustable optical transmission and power conversion efficiency, *Nat. Energy*, 2020, **5**, 468–477, DOI: **10.1038/s41560-020-0624-7**.

3 F. Bella, A. Lamberti, S. Bianco, E. Tresso, C. Gerbaldi and C. F. Pirri, Floating Photovoltaics: Floating, Flexible Polymeric Dye-Sensitized Solar-Cell Architecture: The Way of Near-Future Photovoltaics, *Adv. Mater. Technol.*, 2016, **1**, 1600002, DOI: **10.1002/admt.201670011**.

4 Q. Yu, Y. Wang, Z. Yi, N. Zu, J. Zhang, M. Zhang and P. Wang, High-efficiency dye-sensitized solar cells: The influence of lithium ions on exciton dissociation, charge recombination, and surface states, *ACS Nano*, 2010, **4**(10), 6032–6038, DOI: **10.1021/nn101384e**.

5 P. Karthika and S. Ganesan, Poly(Ethylene Glycol)-Poly(Propylene Glycol)-Poly(Ethylene Glycol) and Polyvinylidene Fluoride Blend Doped with Oxydianiline-Based Thiourea Derivatives as a Novel and Modest Gel Electrolyte System for Dye-Sensitized Solar Cell Applications, *RSC Adv.*, 2020, **10**(25), 14768–14777, DOI: **10.1039/d0ra01031f**.

6 N. M. Saidi, N. K. Farhana, S. Ramesh and K. Ramesh, Influence of different concentrations of 4-*tert*-butyl-pyridine in a gel polymer electrolyte towards improved performance of Dye-Sensitized Solar Cells (DSSC), *Sol. Energy*, 2021, **216**, 111–119, DOI: **10.1016/j.solener.2020.12.058**.

7 F. I. Chowdhury, J. Islam, A. K. Arof, M. U. Khandaker, H. M. Zabed, I. Khalil and J. Uddin, Electrocatalytic and structural properties and computational calculation of PAN-EC-PC-TPAI-I₂gel polymer electrolytes for dye sensitized solar cell application, *RSC Adv.*, 2021, **11**, 22937–22950, DOI: **10.1039/d1ra01983**.

8 M. O. S. Lobregas and D. H. Camacho, Gel polymer electrolyte system based on starch grafted with ionic liquid: Synthesis, characterization and its application in dye-sensitized solar cell, *Electrochim. Acta*, 2019, **298**(1), 219–228, DOI: **10.1016/j.electacta.2018.12.090**.

9 F. Bella, A. Sacco, G. P. Salvador, S. Bianco, E. Tresso, C. F. Pirri and R. Bongiovanni, First Pseudohalogen Polymer Electrolyte for Dye-Sensitized Solar Cells Promising for In Situ Photopolymerization, *J. Phys. Chem. C*, 2013, **117**(40), 20421–20430, DOI: **10.1021/jp405363x**.

10 X.-Z. Chen, W.-J. He, L.-X. Ding, S.-Q. Wangand and H.-H. Wang, Enhancing interfacial contact in all solid state batteries with a cathode-supported solid electrolyte membrane framework, *Energy Environ. Sci.*, 2019, **12**, 938–944, DOI: **10.1039/C8EE02617C**.

11 F. Bella, J. Popovic, A. Lamberti, E. Tresso, C. Gerbaldi and J. Maier, Interfacial Effects in Solid–Liquid Electrolytes for Improved Stability and Performance of Dye-Sensitized Solar Cells, *ACS Appl. Mater. Interfaces*, 2017, **9**, 37797–37803, DOI: **10.1021/acsami.7b11899**.

12 J. M. Abisharani, S. Balamurugan, A. Thomas, S. Devikala, M. Arthanareeswari, S. Ganesan and M. Prakash, Incorporation of organic additives with electron rich donors (N, O, S) in gelatin gel polymer electrolyte for dye sensitized solar cells, *Sol. Energy*, 2021, **218**, 552–562, DOI: **10.1016/j.solener.2021.03.007**.

13 A. Azmar, R. H. Y. Subbana and T. Winie, Improved long-term stability of dye-sensitized solar cell employing PMA/PVAc based gel polymer electrolyte, *Optical Mater.*, 2019, **96**, 109349, DOI: **10.1016/j.optmat.2019.109349**.

14 M. S. Suait, F. N. Jumaah, H. M. Faizzia, S. Mamat, N. A. Ludin, W. A. Farhan, A. Haron, N. Atifah, M. N. Latif, K. H. Badri and A. Ahmad, Palm-based polyurethane-ionic liquid gel polymer electrolyte for quasi-solid state dye sensitized solar cell, *Industrial Crops & Products*, 2018, **113**, 406–413, DOI: **10.1016/j.indcrop.2018.01.008**.

15 S. Balamurugan, S. Ganesan, S. Kamaraj, V. Mathew, J.-K. Kim, N. Arumugam and A. I. Almansour, Effect of poly (ethylene glycol) gel polymer electrolyte consist of novel heteroleptic cobalt redox shuttle and pyridine based organic additive on performance of dye sensitized solar cells, *Optical Mater.*, 2022, **125**, 112082, DOI: **10.1016/j.optmat.2022.112082**.

16 K. M. Masud, K. M. Kim and H. K. Kim, Polymer Gel Electrolytes Based on PEG-Functionalized ABA Triblock Copolymers for Quasi-Solid-State Dye-Sensitized Solar Cells: Molecular Engineering and Key Factors, *ACS Appl. Mater. Interfaces*, 2020, **12**(37), 42067–42080, DOI: **10.1021/acsami.0c09519**.

17 R. S. Seni, N. Puspitasari and Endarko, Effect of The Addition of PEG and PVA Polymer for Gel Electrolytes in Dye-Sensitized Solar Cell (DSSC) with Chlorophyll as Dye Sensitizer, *IOP Conf. Ser.: Mater. Sci. Eng.*, 2017, **214**, 012011, DOI: **10.1088/1757-899X/214/1/012011**.

18 W. C. Lai, L. J. Liu and P. H. Huang, Novel Composite Gel Electrolytes with Enhanced Electrical Conductivity and Thermal Stability Prepared Using Self-Assembled Nanofibrillar Networks, *Langmuir*, 2017, **33**, 6390–6397, DOI: **10.1021/acs.langmuir.7b01053**.

19 K. Sing Liow, C. S. Sipaut, R. Fran Mansa, M. Ching Ung and S. Ebrahimi, Effect of PEG Molecular Weight on the Polyurethane-Based Quasi-Solid-State Electrolyte for Dye-Sensitized Solar Cells, *Polymers*, 2022, **14**, 3603, DOI: **10.3390/polym14173603**.

20 L. Kai Sing, C. Stephen Sipaut, R. Fran Mansa and J. Dayou, Dye Sensitized Solar Cell Based on Polyethylene Glycol/4,4'-Diphenylmethane Diisocyanate Copolymer Quasi Solid State Electrolyte, *Appl. Mech. Mater.*, 2014, **625**, 140–143, DOI: **10.4028/www.scientific.net/AMM.625.140**.

21 Masud, K.-M. Kim and H.-K. Kim, Highly efficient gel electrolytes by end group modified PEG-based ABA triblock copolymers for quasi-solid-state dye-sensitized solar cells, *Chem. Eng. J.*, 2021, **420**(1), 129899, DOI: **10.1016/j.cej.2021.129899**.

22 J. Gong, K. Sumathy and J. Liang, Polymer electrolyte based on polyethylene glycol for quasi-solid state dye sensitized solar cells, *Renewable Energy*, 2012, **39**, 419–423, DOI: **10.1016/j.renene.2011.07.015**.

23 R. Kushwaha, P. Srivastava and L. Bahadur, Ionic liquid integrated polyethylene glycol (PEG)-based quasi-solid electrolyte for efficiency enhancement of dye-sensitized solar cell, *J. Solid State Electrochem.*, 2017, **21**, 1533–1543, DOI: **10.1007/s10008-017-3517-3**.

24 Q.-H. Li, H.-Y. Chen, L. Lin, P.-J. Li, Y.-C. Qin, M.-J. Li, B.-L. He, L. Chu and Q.-W. Tang, Quasi-solid-state dye-sensitized solar cell from polyaniline integrated poly(hexamethylene diisocyanate tripolymer/polyethylene glycol) gel electrolyte, *J. Mater. Chem. A*, 2013, **1**, 5326–5332, DOI: **10.1039/C3TA10224F**.

25 K. M. Kim, Masud, J.-M. Ji and H.-K. Kim, PAN-Based Triblock Copolymers Tailor-Made by Reversible Addition–-Fragmentation Chain Transfer Polymerization for HighPerformance Quasi-Solid State Dye-Sensitized Solar Cells, *ACS Appl. Energy Mater.*, 2021, **4**(2), 1302–1312, DOI: **10.1021/acsaem.0c02545**.

26 A. K. Arof, I. M. Noor, M. H. Buraidah, T. M. W. J. Bandara, M. A. Careem, I. Albinsson and B.-E. Mellander, Polyacrylonitrile gel polymer electrolyte based dye sensitized solar cells for a prototype solar panel, *Electrochim. Acta*, 2017, **251**, 223–234, DOI: **10.1016/j.electacta.2017.08.129**.

27 C.-L. Chen, H.-S. Teng and Y.-L. Lee, Preparation of highly efficient gel-state dye-sensitized solar cells using polymer gel electrolytes based on poly(acrylonitrile-*co*-vinyl acetate), *J. Mater. Chem.*, 2011, **21**, 628–632, DOI: **10.1039/C0JM03597A**.

28 F. Bella, J. Popovic, A. Lamberti, E. Tresso, C. Gerbaldi and J. Maier, Interfacial Effects in Solid-Liquid Electrolytes for Improved Stability and Performance of DyeSensitized Solar Cell, *ACS Appl. Mater. Interfaces*, 2017, **9**(43), 37797–37803, DOI: **10.1021/acsami.7b11899**.

29 D. Pugliese, A. Lamberti, F. Bella, A. Sacco, S. Bianco and E. Tresso, TiO$_2$ nanotubes as flexible photoanode for back-illuminated dye-sensitized solar cells with hemi-squaraine organic dye and iodine-free transparent electrolyte, *Org. Electron.*, 2014, **15**(12), 3715–3722, DOI: **10.1016/j.orgel.2014.10.018**.

30 A. Bist and S. Chatterjee, Review on Efficiency Enhancement Using Natural Extract Mediated Dye-Sensitized Solar Cell for Sustainable Photovoltaics, *Energy Technol.*, 2021, **9**, 2001058, DOI: **10.1002/ente.202001058**.

31 N. Ahmad, J. Vunduk, A. Klaus, N. Y. Dahlan, S. Ghosh, L. Dufossé, N. A. Bani and W. A. Al Qadr Imad, Roles of Medicinal Mushrooms as Natural Food Dyes and Dye-Sensitised Solar Cells (DSSC): Synergy of Zero Hunger and Affordable Energy for Sustainable Development, *Sustainability*, 2022, **14**(21), 13894, DOI: **10.3390/su142113894**.

32 M. Sethupathy, P. Pandey and P. Manisankar, Photovoltaic performance of dye-sensitized solar cells fabricated with polyvinylidene fluoride-polyacrylonitrile-silicondioxide hybrid composite membrane, *Mater. Chem. Phys.*, 2014, **143**, 1191–1198, DOI: **10.1016/j.matchemphys.2013.11.020**.

33 T. M. W. J. Bandara, W. J. M. J. S. R. Jayasundara, H. D. N. S. Fernando, M. A. K. L. Dissanayake, L. A. A. De Silva, P. S. L. Fernando, M. Furlani and B.-E. Mellander, Efficiency enhancement of dye-sensitized solar cells with PAN:CsI:LiI quasi-solid state (gel) electrolytes, *J. Appl. Electrochem.*, 2014, **44**, 917–926, DOI: **10.1007/s10800-014-0711-1**.

34 E. N. Jayaweera, C. S. K. Ranasinghe, G. R. A. Kumara, W. M. N. M. B. Wanninayake, K. G. C. Senarathne, K. Tennakone, R. M. G. Rajapakse and O. A. Ileperuma, Novel method to improve performance of dye-sensitized solar cells based on quasi-solid gel-polymer electrolytes, *Electrochim. Acta*, 2015, **152**, 360–367, DOI: **10.1016/j.electacta.2014.11.156**.

35 T. M. W. J. Bandara, H. D. N. S. Fernado, M. Furlani, I. Albinsson, M. A. K. L. Dissanayake, J. L. Ratnasekera and B.-E. Mellander, Dependence of solar cell performance on the nature of alkaline counterion in gel polymer electrolytes containing binary iodides, *J. Solid State Electrochem.*, 2017, **21**, 1571–1578, DOI: **10.1007/s10008-017-3518-2**.

36 M. Rayung, M.-M. Aung, M. S. SukorSu'ait, L.-C. Abdullah, A. Ahmad and H.-N. Lim, Performance Analysis of Jatropha Oil-Based Polyurethane Acrylate Gel Polymer Electrolyte for Dye-Sensitized Solar Cells, *ACS Omega*, 2020, **5**(24), 14267–14274, DOI: **10.1021/acsomega.9b04348**.

37 Z. Lan, J. Wu, J. Lin and M. Huang, Quasi-solid-state dye-sensitized solar cells with a novel efficient absorbent for liquid electrolyte based on PAA–PEG hybrid, *J. Power Sources*, 2007, **164**(2), 921–925, DOI: **10.1016/j.jpowsour.2006.11.011**.

38 F. Bella, E. D. Ozzello, S. Bianco and R. Bongiovanni, Photopolymerization of acrylic/methacrylic gel-polymer electrolyte membranes for dye-sensitized solar cells, *Chem. Eng. J.*, 2013, **225**, 873–879, DOI: **10.1016/j.cej.2013.04.057**.

39 F. Bella, D. Pugliese, J. R. Nair, A. Sacco, S. Bianco, C. Gerbaldi, C. Barolo and R. Bongiovanni, A UV-crosslinked polymer electrolyte membrane for quasi-solid dye-sensitized solar cells with excellent efficiency and durability, *Phys. Chem. Chem. Phys.*, 2013, **15**(11), 3706–3711, DOI: **10.1039/C3CP00059A**.

40 Y. Shi, Y. Wang, M. Zhang and X. Dong, Influences of cation charge density on the photovoltaic performance of dye-sensitized solar cells: Lithium, sodium, potassium, and dimethylimidazolium, *Phys. Chem. Chem. Phys.*, 2011, **13**, 14590–14597, DOI: **10.1039/C1CP21020C**.

41 H. Ozawa, Y. Okuyama and H. Arakawa, Effects of cation composition in the electrolyte on the efficiency improvement of black dye-based dye-sensitized solar cells, *RSC Adv.*, 2013, **3**, 9175–9177, DOI: **10.1039/c3ra23495a**.

42 T. M. W. J. Bandara, M. F. Aziz, H. D. N. S. Fernando, M. A. Careem, A. K. Arof and B.-E. Mellander, Efficiency enhancement in dye-sensitized solar cells with a novel PAN-based gel polymer electrolyte with ternary iodides, *J. Solid State Electrochem.*, 2015, **19**(8), 2353–2359, DOI: **10.1007/s10008-015-2857-0**.

43 K. E. Kim, S. R. Jang, J. H. Park, R. Vittal and K. J. Kim, Enhancement in the Performance of Dye-Sensitized Solar Cells Containing ZnO-Covered TiO$_2$ Electrodes Prepared by Thermal Chemical Vapor Deposition, *Solar Energy Mater. & Solar Cells*, 2007, **91**, 366–370, DOI: **10.1016/j.solmat.2006.10.010**.

44 V. M. Mohan, K. Murakami, A. Kono and M. Shimomura, Poly(acrylonitrile)/activated carbon composite polymer gel electrolyte for high efficiency dye sensitized solar cells, *J. Mater. Chem. A*, 2013, **1**, 7399–7407, DOI: **10.1039/C3TA10392G**.

45 V. M. Mohan, K. Murakam, J. Madhavi and V. R. Machavaram, Improved efficiency in dye-sensitized solar cell *via* surface modification of TiO$_2$ photoelectrode by spray pyrolysis, *J. Mater. Sci.: Mater. Electron.*, 2021, **13**, 18231–18239, DOI: 10.1007/s10854-021-06366-8.

46 T. Nazia and V. M. Mohan, Synthesis of organic sulfobetaine-based polymer gel electrolyte for dye-sensitized solar cell application, *Polym. Adv. Technol.*, 2017, **28**(11), 1504–1509, DOI: 10.1002/pat.4028.

47 V. M. Mohan and K. Murakami, Hydrothermal Synthesis of TiO$_2$ Porous Hollow Nanospheres for Coating on the Photoelectrode of Dye-Sensitized Solar Cells, *Jpn. J. Appl. Phys.*, 2012, **51**, 02BP1, DOI: 10.1143/JJAP.51.02BP11.

48 Y. Yang, J. Zhang, C. H. Zhou, S. J. Wu, S. Xu, W. Liu, H. W. Han, B. L. Chen and X. Z. Zhao, Effect of Lithium Iodide Addition on Poly(ethylene oxide)-Poly(vinylidene fluoride) Polymer-Blend Electrolyte for Dye-Sensitized Nanocrystalline Solar Cell, *J. Phys. Chem. B*, 2008, **112**, 6594–6602, DOI: 10.1021/jp801156h.

49 S. Agarwala, C. K. N. Peh and G. W. Ho, Investigation of Ionic Conductivity and Long-Term Stability of a LiI and KI Coupled Diphenylamine Quasi-Solid-State Dye-Sensitized Solar Cell, *ACS Appl. Mater. Interfaces*, 2011, **3**, 2383–2391, DOI: 10.1021/am200296f.

50 V. M. Mohan and K. Murakami, Dye sensitized solar cell withcarbon doped (PAN/PEG) polymer quasi-solid gel electrolyte, *J. Adv. Res.*, 2011, **2**(2), 021112.

51 Y.-J. Jiang and F.-Y. Zhao, Application of Bunchy TiO$_2$ Hierarchical Microspheres as a Scattering Layer for Dye-Sensitized Solar Cells, *Front. Energy Res.*, 2021, **9**, 682709, DOI: 10.3389/fenrg.2021.682709.

52 R. Adel, T. Abdallah and H. Talaat, Efficiency enhancement of photovoltaic performance of dye sensitized solar cell using conducting polymer electrolyte of different functional group, *J. Phys.: Conf. Ser.*, 2019, **1253**, 012029, DOI: 10.1088/1742-6596/1253/1/012029.

53 P. Gnida, M. F. Amin, A. K. Pająk and B. Jarząbek, Polymers in High-Efficiency Solar Cells: The Latest Reports, *Polymers*, 2022, **14**(10), 1946, DOI: 10.3390/polym14101946.

54 R. Na, G. Guo, S.-L. Zhang, P. F. Huo, Y.-L. Du, J.-C. Luan, K. Zhu and G.-B. Wang, A novel poly(ethylene glycol)–grafted poly(arylene ether ketone) blend micro-porous polymer electrolyte for solid-state electric double layer capacitors formed by incorporating a chitosan-based LiClO4 gel electrolyte, *J. Mater. Chem. A*, 2016, **4**, 18116–18127, DOI: 10.1039/C6TA07846J.

55 J. Kim, Y.-G. Choi, Y.-H. Ahn, D.-J. Kim and J.-H. Par, Optimized ion-conductive pathway in UV-cured solid polymer electrolytes for all-solid lithium/sodium ion batteries, *J. Membr. Sci.*, 2021, **617**, 118771, DOI: 10.1016/j.memsci.2020.118771.

56 A. K. Bharwal, L. Manceriu, C. Iojoiu, J. Dewalque, T. Toupance, L. Hirsch, C. Henrist and F. Alloin, Ionic Liquid-like Polysiloxane Electrolytes for Highly Stable Solid-State Dye-Sensitized Solar Cells, *ACS Appl. Energy Mater.*, 2018, **1**(8), 4106–4114, DOI: 10.1021/acsaem.8b00769.

57 S. Srivishnu, S. P. Kumar and L. Giribabu, Cu(II/I) redox couples: potential alternatives to traditional electrolytes for dye-sensitized solar cells, *Chemistry Mater. Adv.*, 2021, **2**, 1229–1247, DOI: 10.1039/d0ma01023e.

58 A. Gunasekaran, A. Sorrentino, A. M. Asiri and S. Anandan, Guar gum-based polymer gel electrolyte for dye-sensitized solar cell applications, *Sol. Energy*, 2020, **208**, 160–165, DOI: 10.1016/j.solener.2020.07.084.

59 W. Naim, V. Novelli, I. Nikolinakos, N. Barbero, I. Dzeba, F. Grifoni, Y.-M. Ren, T. Alnasser, A. Velardo, R. Borrelli, S. H. Shaik, M. Zakeeruddin, M. Graetzel, C. Barolo and F. Sauvage, Transparent and Colorless Dye-Sensitized Solar Cells Exceeding 75% Average Visible Transmittance, *JACS*, 2021, **1**, 409–426, DOI: 10.1021/jacsau.1c00045.

60 P. Ma, Y. Y. Fang, A. Li, B.-X. Wen, H.-B. Cheng, X.-W. Zhou, Y.-M. Shi, H.-Y. Yang and Y. Lin, Highly efficient and stable ionic liquid-based gel electrolytes, *Nanoscale*, 2021, **13**, 7140–7151, DOI: 10.1039/d0nr08765c.

61 F. S. Lin, M. Sakthivel, M.-S. Fan, J.-J. Lin, R.-J. Jeng and K.-C. Ho, A novel multifunctional polymer ionic liquid as an additive in iodide electrolyte combined with silver mirror coating counter electrodes for quasi-solidstate dye-sensitized solar cells, *J. Mater. Chem. A*, 2021, **9**, 4907–4921, DOI: 10.1039/D0TA10826J.

62 P. Manafia, H. Nazockdast, M. Karimi, M. Sadighi and L. Magagnin, A study on the microstructural development of gel polymer electrolytes and different imidazolium-based ionic liquids for dye-sensitized solar cells, *J. Power Sources*, 2021, **481**, 228622, DOI: 10.1016/j.jpowsour.2020.228622.

63 C. Li, C.-H. Xin, L. Xu, Y. Zhong and W.-J. Wu, Components control for high-voltage quasi-solid state dye-sensitized solar cells based on two-phase polymer gel electrolyte, *Sol. Energy*, 2019, **181**, 130–136, DOI: 10.1016/j.solener.2019.01.072.

64 J. C. de Haro, E. Tatsi, L. Fagiolari, M. Bonomo, C. Barolo, S. Turri, F. Bella and G. Griffini, Lignin-Based Polymer Electrolyte Membranes for Sustainable Aqueous Dye-Sensitized Solar Cells, *ACS Sustainable Chem. Eng.*, 2021, **9**, 8550–8560, DOI: 10.1021/acssuschemeng.1c01882.

65 S. K. Ahn, T. W. Ban, P. Sakthivel, J. W. Lee, Y. S. Gal, J. K. Lee, M. R. Kim and S. H. Jin, Development of Dye-Sensitized Solar Cells Composed of Liquid Crystal Embedded, ElectrospunPoly(vinylidene fluoride-*co*-hexafluoropropylene) Nanofibers as Polymer Gel Electrolytes, *ACS Appl. Mater. Interfaces*, 2012, **4**, 2096–2100, DOI: 10.1021/am3000598.

66 V. Novelli, N. Barbero, C. Barolo, G. Viscardi, M. Sliwa and F. Sauvage, Electrolyte containing lithium cation in squaraine-sensitized solar cells: Interactions and consequences for performance and charge transfer dynamics, *Phys. Chem. Chem. Phys.*, 2017, **19**, 27670–27681, DOI: 10.1039/C7CP04340F.

67 T. He, L. Wang, F. Fabregat-Santiago, G. Liu, Y. Li, C. Wang and R. Guan, Electron trapping induced electrostatic adsorption of cations: a general factor leading to photoactivity decay of nanostructured TiO$_2$, *J. Materials Chemistry A*, 2017, **5**, 6455–6464, DOI: 10.1039/C7TA01132F.

68 N. Mariotti, M. Bonomo, L. Fagiolari, N. Barbero, C. Gerbaldi, F. Bella and C. Barolo, Recent advances in

eco-friendly and cost-effective materials towards sustainable dye-sensitized solar cells, *Green Chem.*, 2020, **22**, 7168–7218, DOI: **10.1039/D0GC01148G**.

69 M. A. K. L. Dissanayake, C. A. Thotawatthage, G. K. R. Senadeera, T. M. W. J. Bandara, W. J. M. J. S. R. Jayasundera and B.-E. Mellander, Efficiency enhancement by mixed cation effect in dye-sensitized solar cells with PAN based gel polymer electrolyte, *J. Photochem. Photobiol. A Chem.*, 2012, **246**, 29–35, DOI: **10.1016/j.jphotochem.2012.06.023**.

70 M. A. K. L. Dissanayake, C. A. Thotawatthage, G. K. R. Senadeera, T. M. W. J. Bandara, W. J. M. J. S. R. Jayasundara and B.-E. Mellander, Efficiency enhancement in dye sensitized solar cells based onPAN gel electrolyte with Pr4NI + MgI2 binary iodide salt mixture, *J. Appl. Electrochem.*, 2013, **43**, 891–901, DOI: **10.1007/s10800-013-0582-x**.

71 T. M. W. J. Bandara, W. J. M. J. S. R. Jayasundara, M. A. K. L. Dissanayake, D. N. S. Fernando, M. Furlani, I. Albinsson and B.-E. Mellander, Quasi solid state polymer electrolyte with binary iodide salts for photo-electrochemical solar cells, *Int. J. Hydrog Energy*, 2014, **39**, 2997–3004, DOI: **10.1016/j.ijhydene.2013.05.163**.

72 S. Venkatesan, S.-C. Su, W.-N. Hung, I.-P. Liu, H. Teng and Y.-L. Lee, Printable electrolytes based on polyacrylonitrile and gamma-butyrolactone for dye-sensitized solar cell application, *J. Power Sources*, 2015, **298**, 385–390, DOI: **10.1016/j.jpowsour.2015.07.062**.

73 J. W. Chew, M. H. Khanmirzaei, A. Numan, F. S. Omar, K. Ramesh and S. Ramesh, Performance studies of ZnO and multi walled carbon nanotubes-based counter electrodes with gel polymer electrolyte for dye-sensitized solar cell, *Mater. Sci. Semicond. Process.*, 2018, **83**, 144–149, DOI: **10.1016/j.mssp.2018.04.036**.